Scientific Research Publishing

Journal of Electromagnetic Analysis and Applications, 2026, 18(2), 29-43
https://www.scirp.org/journal/jemaa
ISSN Online: 1942-0749
ISSN Print: 1942-0730

Investigation of the Effects of Geometric Parameters on Cogging Torque and Efficiency in Brushless DC Motors

Hakan Citak[1], Huseyin Gunes[2], Sabri Bicakci[3], Mustafa Coramik[4], Yavuz Ege[4*]

[1]Department of Electric and Energy, Balikesir Vocational High School, Balıkesir University, Balıkesir, Türkiye
[2]Department of Computer Engineering, Faculty of Engineering, Balıkesir University, Balıkesir, Türkiye
[3]Department of Electric and Electronics Engineering, Faculty of Engineering, Balıkesir University, Balıkesir, Türkiye
[4] Department of Physics, Necatibey Faculty of Education, Balikesir University, Balıkesir, Türkiye
Email: hcitak@balikesir.edu.tr, hgunes@balikesir.edu.tr, sbicakci@balikesir.edu.tr, *yege@balikesir.edu.tr, mustafacoramik@balikesir.edu.tr

How to cite this paper: Citak, H., Gunes, H., Bicakci, S., Coramik, M. and Ege, Y. (2026) Investigation of the Effects of Geometric Parameters on Cogging Torque and Efficiency in Brushless DC Motors. *Journal of Electromagnetic Analysis and Applications*, **18**, 29-43.
https://doi.org/10.4236/jemaa.2026.182002

Received: January 24, 2026
Accepted: February 10, 2026
Published: February 13, 2026

Abstract

In this study, the effects of critical geometric design parameters on the performance characteristics of Brushless Direct Current (BLDC) motors are investigated. Using the Finite Element Method (FEM), the effects of magnet thickness, pole embrace, and stator slot geometry were analyzed on a reference BLDC motor model selected for applications requiring high power density and efficiency. Parametric simulations conducted within the ANSYS Maxwell environment were optimized by taking into account magnetic saturation and air gap flux distribution. The analysis results demonstrate that motor performance and torque quality can be maximized without incurring additional material costs by determining the optimum saturation point for magnet thickness, selecting a pole embrace of 0.75, and modifying the stator slot geometry. Through this optimization, cogging torque was reduced by 94.01% compared to the reference model, thereby directly enhancing the acoustic comfort and mechanical lifespan of the motor. The limited variation of 1.67% in efficiency was successfully managed within a reasonable "Optimization Balance" favouring driving quality, attributed to the smoothness of torque transmission and the weight advantage gained from motor weight reduction.

Keywords

Brushless DC (BLDC) Motor, Geometric Optimization, Cogging Torque, Finite Element Analysis (FEA), Efficiency

1. Introduction

Brushless Direct Current (BLDC) motors have emerged as the cornerstone of modern electromechanical systems, owing to their superior advantages over conventional brushed motors, such as high torque-to-weight ratio, extended service life, and ease of maintenance. Pioneering research regarding driver topologies and dynamic characteristics has accelerated the industrial adoption of this motor technology [1] [2]. Currently, they occupy a central role in energy-efficiency-oriented designs across a broad spectrum of applications, ranging from electric bicycles to hybrid vehicles [3]. However, one of the primary inherent disadvantages of BLDC motors is torque ripple, referred to in the literature as "cogging torque", which arises from the magnetic interaction between the permanent magnets and the stator teeth [4]. These fluctuations induce noise and vibration, particularly within asymmetric air gaps, thereby adversely affecting the acoustic comfort and mechanical lifespan of the motor [5] [6].

Geometric optimization studies aimed at maximizing motor performance predominantly focus on the stator structure. The modification of stator slot shape is widely regarded as one of the most effective methods for mitigating cogging torque [7]. However, the combination of stator slot and pole numbers, along with the selection of coil diameters, has a direct impact on the motor's efficiency and stability [8] [9]. Another common method employed on the stator side is stator skewing; this technique enhances the back-EMF waveform while suppressing torque ripples [10]. Furthermore, recently developed auxiliary slot techniques regulate magnetic flux paths, thereby facilitating smoother motor operation [11].

Rotor geometry and magnet placement are also critical parameters influencing performance. In surface-mounted permanent magnet (SPM) motors, optimizing rotor magnetic displacements is a frequently employed method to enhance torque quality [12] [13]. Altering the ratio of magnet pole arc to pole pitch optimizes air gap flux density, thereby influencing the motor's output power [14]. Additionally, grooving operations performed on rotor poles and the modification of magnet shape minimize harmonic components [15] [16]. In Interior Permanent Magnet (IPM) motors, optimizing the rotor shape according to the direction of magnetization and utilizing tangential placements provide high torque density, particularly for hybrid vehicle applications [17] [18].

In advanced design approaches, various motor topologies and material properties are also taken into consideration. For instance, in studies comparing slotted and slotless stator structures, the advantages of slotless designs for high-speed applications are highlighted [19]. Similarly, specialized magnet configurations, such as the Halbach array, and geometries providing flux concentration increase the power density of the motor [20] [21]. However, as these high-performance designs entail high thermal loads, the selection of stator materials requires support through thermal analyses [22].

Currently, software utilizing the Finite Element Method (FEM) (e.g., ANSYS Maxwell) and multivariate optimization algorithms such as Taguchi have become

standard for analyzing the complex interactions of all these geometric parameters [23] [24]. Furthermore, the online identification of motor parameters is crucial for minimizing the effects of manufacturing tolerances that are unforeseen during the design phase [25]. The primary objective of this study is to optimize the geometric parameters of a reference BLDC motor model to meet the high-power density and efficiency criteria required for electric bicycles. Accordingly, the effects of magnet thickness, pole embrace, and stator slot geometry on the performance of a BLDC motor with a stator outer diameter of 200 mm, an inner diameter of 160 mm, and a height of 24 mm are investigated in detail. The critical roles of these specified design variables on the motor's operational efficiency were analyzed using the Finite Element Method (FEM), and the resulting data were examined through a holistic approach. These comprehensive analyses are significant for determining the optimal motor design parameters to maximize energy efficiency in electric transportation vehicles and for contributing to the domestic design literature.

2. Material and Method

In this study, the Finite Element Method (FEM) was employed to investigate the effects of geometric parameters on the efficiency and torque characteristics of the Brushless Direct Current (BLDC) motor used in electric bicycles. The analyses were conducted within the ANSYS Maxwell environment, which is widely utilized in the field of electromagnetic design and simulation. The parametric design process using RMxprt, which constitutes the initial stage of the BLDC motor design workflow, is a critical phase where the mathematical framework of the motor is established. In this phase, by proceeding directly with numerical data rather than geometric drawings, the machine type is selected as BLDC, and basic dimensions such as the stator outer diameter, inner diameter, and stack length, along with the number and type of slots, are determined. Subsequently, the number of poles, magnet configuration, and dimensions are defined within the rotor structure, while electrical parameters such as wire diameter and number of turns, as well as appropriate steel sheet and magnet types from the material library, are selected in the winding section. Finally, the analysis process is completed, and analytical torque, speed, and efficiency curves are obtained (**Figure 1**).

2.1. Reference Motor Design and Specifications

The motor selected as a reference is an outer-rotor BLDC motor designed for electric bicycle applications. The fundamental electrical and mechanical parameters of the motor utilized in the study were established in full compliance with current industrial manufacturing standards and commercial reference models; these technical data were defined within the ANSYS Maxwell for analysis. This reference motor was employed as a "base model" to benchmark the effects of geometric modifications.

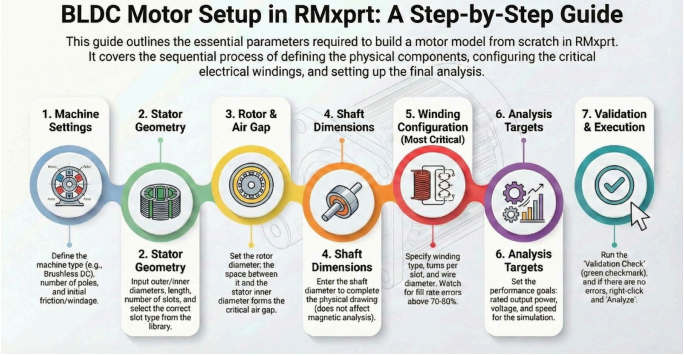

Figure 1. BLDC motor design process.

2.1.1. Stator Setup

In the RMxprt module within ANSYS Maxwell, stator design is one of the most fundamental stages determining the magnetic circuit and winding structure of the motor. Principal dimensions defined in this section, such as outer diameter, inner diameter, and stack length, constitute the physical framework that directly influences the total power density of the motor (**Figure 2**). In addition to dimensional parameters, the selection of the number of stator slots and their geometry is of critical importance regarding magnetic flux distribution and tooth saturation (**Figure 3**). During the design process, the winding structure and the magnetic characteristics of the selected steel material (Steel-1008) are defined in the system, ensuring that the analytical model yields result that most closely approximate real physical behaviour (**Figure 4**).

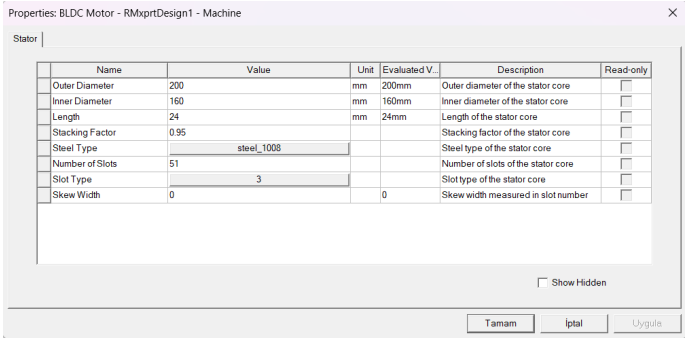

Figure 2. Definition of the main dimensions of the BLDC motor.

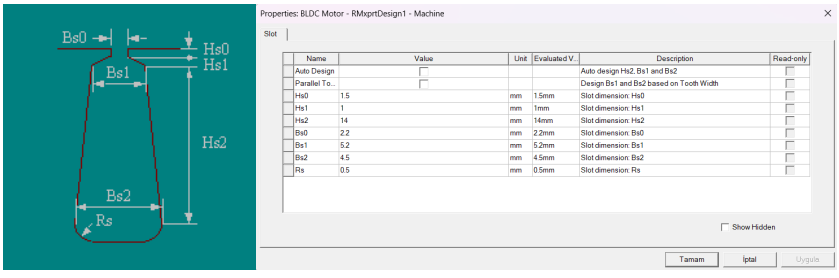

(a) (b)

Figure 3. (a) Slot geometry of the BLDC motor, (b) Definition of slot parameter dimensions.

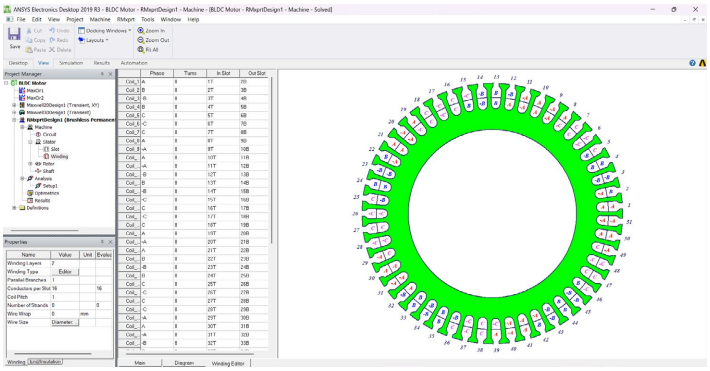

Figure 4. Winding structure of the BLDC motor.

2.1.2. Rotor Setup

In the RMxprt module of ANSYS Maxwell, rotor setup is one of the most critical stages determining the motor's dynamic performance and torque production capacity. In this section, the number of poles is determined first, establishing the fundamental relationship between the motor's electrical frequency and mechanical speed. After selecting the magnet configuration (surface-mounted or embedded structure) in the rotor design, parameters such as magnet thickness and pole embrace are input to optimize the magnetic flux density in the air gap (**Figure 5**). Additionally, the operational stability of the motor under nominal load is analytically ensured by defining the rotor's inner and outer diameters alongside the thermal and magnetic characteristics of the utilized magnet material (NdFe35).

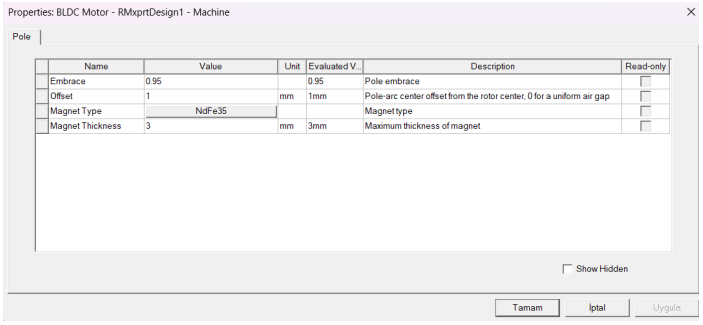

(a)

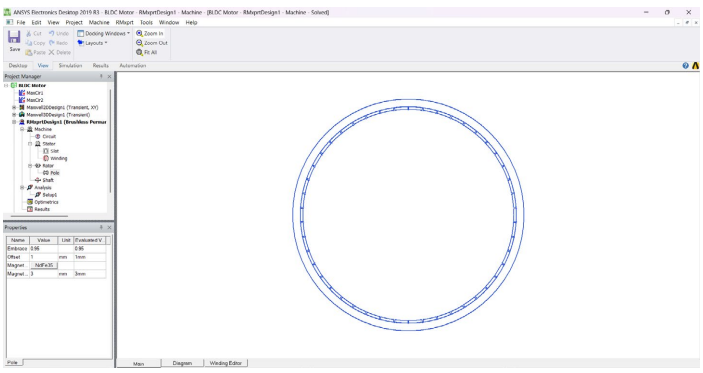

(a)

Figure 5. (a) Definition of rotor parameter values, (b) view of the BLDC motor rotor.

2.1.3. Winding Setup

In the RMxprt module of ANSYS Maxwell, the winding setup is the section where the circuit transforming the motor's electrical input parameters into mechanical output is designed. At this stage, fundamental variables such as conductor wire diameter and the number of turns per coil are determined in accordance with the motor's supply voltage and current density limits. While RMxprt allows for the definition of complex structures such as the number of winding layers and parallel branches, the winding layout can be generated automatically or configured manually according to specific design requirements (**Figure 6**). By optimizing parameters such as the selection of conductor material and fill factor, the objective is to achieve the high efficiency values required in electric bicycle applications by minimizing the motor's copper losses.

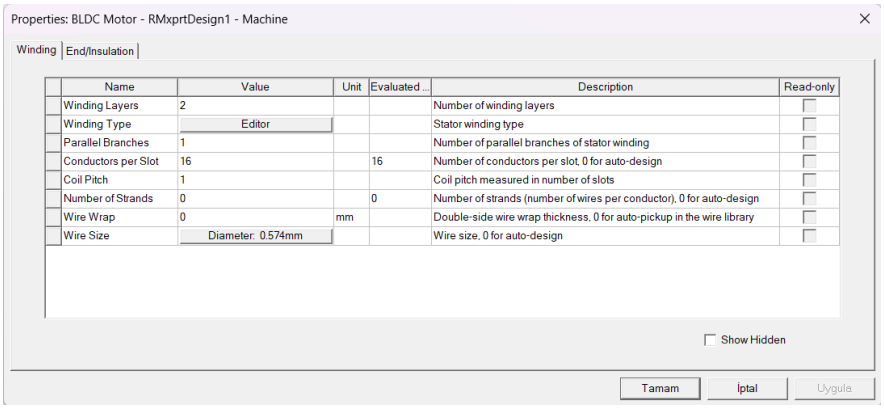

Figure 6. Definition of winding parameter values of the BLDC motor.

2.1.4. Analysis Stage

After geometric and electrical definitions are completed in the ANSYS Maxwell RMxprt module, the "Analyze" stage is initiated to evaluate the design's performance (**Figure 7**). During this process, the software solves the input parameters using analytical magnetic circuit equations, generating critical data such as the motor's torque-speed curve, efficiency map, current values, and power output. The primary advantage provided by RMxprt analysis is that it enables the designer to rapidly assess whether the motor meets the targeted torque and efficiency values. Should the obtained analytical results fall short of the determined criteria, the fundamental framework of the design is refined through parametric optimizations at this stage, prior to proceeding to the more detailed and time-consuming Finite Element Method (FEM)-based Maxwell analyses.

2.2. Finite Element Model and Boundary Conditions

The electromagnetic performance of the BLDC motor was analyzed using the Transient magnetic solver within the ANSYS Maxwell. This solver precisely calculates the time-varying magnetic flux distribution dependent on rotor motion, torque ripples, and induced Back-EMF voltages in the time domain. The following boundary conditions and assumptions were applied in the simulation settings:

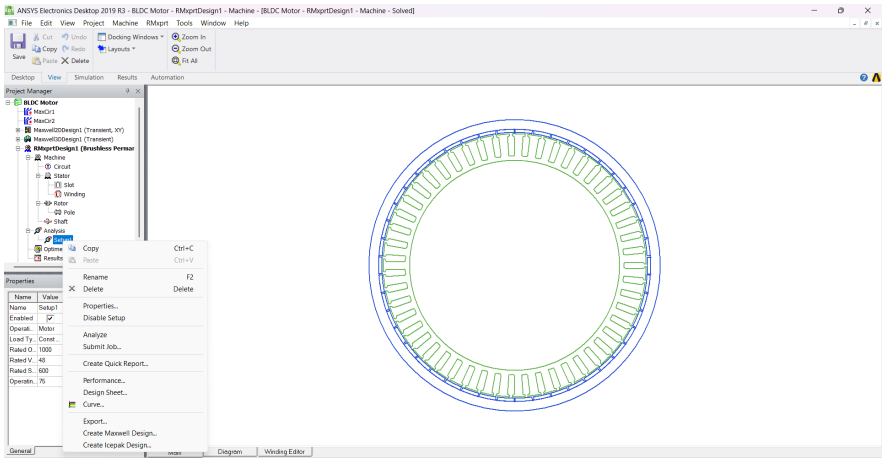

Figure 7. Analysis stage.

- *Material Assignment*: Steel-1008 silicon steel sheet material with known magnetic saturation characteristics was defined for the stator and rotor cores, high-energy density NdFe35 for the permanent magnets, and copper material for the windings.
- *Meshing*: To enhance calculation accuracy, the mesh structure was refined (Mesh refinement), particularly in regions with intense magnetic flux variation such as the air gap, magnet edges, and stator tooth tips. The maximum element length in the air gap was limited to 0.1 mm.
- *Motion Setup*: The rotor speed was set to a constant 600 rpm, and the simulation duration (stop time) and time step were optimized to collect data over a full electrical period.

2.3. Geometric Optimization and Parametric Analysis

A parametric sweep was conducted on fundamental geometric parameters to maximize the efficiency of the BLDC motor and minimize torque ripple. The sequential One-Factor-At-A-Time (OFAT) approach was used in the optimization process. The variables modified during the optimization process are as follows:

1) *Magnet Thickness*: The thickness was varied between 1 mm and 3 mm to determine the balance of magnet volume regarding cost and performance.

2) *Pole Embrace*: The range of 0.65 to 0.95 was scanned, as the ratio of the magnet arc to the pole pitch determines the waveform (square or sinusoidal) of the air gap flux density.

3) *Stator Slot Opening* (*Bs*0): The Stator Slot Opening, which directly affects reluctance, was investigated within the range of 1 mm to 3 mm, considering mechanical tolerances.

In order to validate the resistance values and magnetic properties used in efficiency calculations, a thermal boundary condition of 75˚C, representing steady-state operation, was assumed in the analyses. Under this temperature setting, the performance parameters of the BLDC motor were determined for each geometric variation, and the efficiency (η) was calculated by the RMxprt analysis using Equation (1).

$$\eta = \frac{P_{out}}{P_{out} + P_{cu} + P_{core} + P_{mech}} \times 100 \quad (1)$$

Here, P_{out} represents the output power, P_{cu} the copper losses, P_{core} the core losses, and P_{mech} the mechanical friction losses. The geometric combination yielding the highest efficiency and the lowest cogging torque was designated as the final design.

3. Findings

In this section, the numerical data obtained following the Finite Element Analysis (FEA) procedures, the methodology of which was detailed in Section 2, are presented, and the effects of the determined geometric parameters on motor performance are comprehensively discussed. Parametric sweeps and sensitivity analyses conducted on the reference motor model have demonstrated, through numerical evidence, the critical roles of magnet thickness, pole embrace ratio, and stator slot geometry on the motor's cogging torque and total efficiency characteristics. The direct and indirect effects of each analyzed design variable on performance outputs are examined in the subsections from the perspective of optimized motor design for electric bicycle applications.

3.1. Effect of Magnet Thickness on Torque and Saturation

Magnet thickness, which directly affects the reluctance of the rotor magnetic circuit, was analyzed within the range of 1 mm to 3 mm in 1 mm increments. Simulation results indicate that the increase in magnet thickness initially increases the air gap flux density and, consequently, the average output torque with a linear characteristic.

On the other hand, an examination of the data in Table 1 and Figures 8(a)-(c) reveals that the rate of torque increase tends to diminish as the magnet thickness exceeds 3 mm. This phenomenon can be attributed to magnetic saturation occurring in the stator teeth and the yoke region. This is because the saturated stator core fails to efficiently transmit the increasing magnetomotive force (MMF), leading to magnetic flux leakage. Consequently, in terms of cost and performance optimization, the 3 mm thickness was evaluated as a "knee point" and selected as the optimal value. In summary, these torque-speed (Figures 8(a)-(c)) and flux density characteristics (Figures 8(d)-(f)), obtained across different magnet thicknesses, constitute a fundamental reference for both literature and practice in determining the parameters that provide the most suitable torque values for the operating conditions of electric bicycles.

Table 1. Effect of magnet thickness on Air-Gap Flux Density, Output Torque, and Efficiency.

Magnet thickness (mm)	Air-Gap Flux Density (T)	Output Torque (N·m)	Efficiency (%)
1	0.71824	193.960	84.8922
2	0.85258	294.156	88.3854
3	0.91150	337.427	89.1970

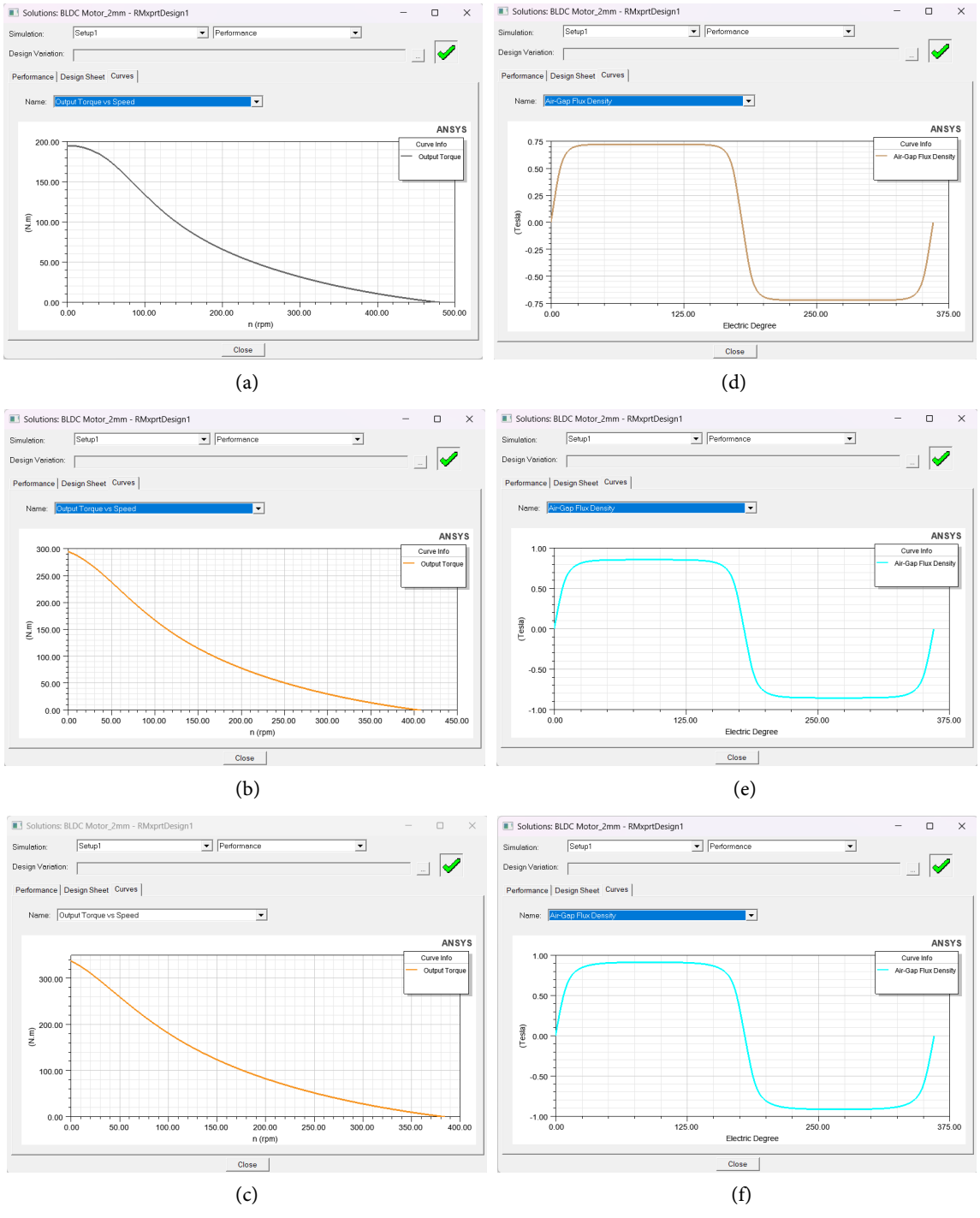

Figure 8. Effects of different magnet thicknesses on performance: (a)-(c) Variation of output torque with revolutions per minute (1, 2, 3 mm), (d)-(f) Air gap flux density characteristics (1, 2, 3 mm).

3.2. Effect of Pole Embrace on Cogging Torque

Cogging torque is the most critical parameter that must be minimized to ensure the quiet and vibration-free operation of the motor. In analyses conducted by varying the ratio of the magnet arc angle to the pole pitch, the effect of this ratio on torque ripple was investigated.

Increasing the pole embrace ratio from 0.65 to 0.80 yielded a 3.57% improvement in average torque by enhancing the effective flux. However, as the pole embrace ratio approaches the full pole pitch, it intensifies the magnetic interaction (reluctance change) between the magnet edges and the stator slot openings, resulting in a significant increase in cogging torque (Table 2 and Figures 9(a)-(c)).

As a result of the analyses, a pole embrace ratio of 0.75 was determined to be the optimal point where a performance balance is achieved; at this value, cogging torque is maintained within acceptable limits (0.0007 N·m peak-to-peak) without compromising average torque production. It was observed that at this ratio, the air gap flux density distribution exhibited a smoother profile, becoming free of harmonic components (Figures 9(d)-(f)); correspondingly, the Back-EMF waveform approached a sinusoidal form, and the Total Harmonic Distortion (THD) rate was significantly reduced.

Table 2. Effect of pole embrace ratio on Cogging Torque, Output Torque, and Efficiency.

Pole Embrace	Cogging Torque (N·m)	Output Torque (N·m)	Efficiency (%)
0.65	0.000144638	327.831	88.2921
0.80	0.000434462	339.542	88.9486
0.95	0.002759850	337.427	89.1970

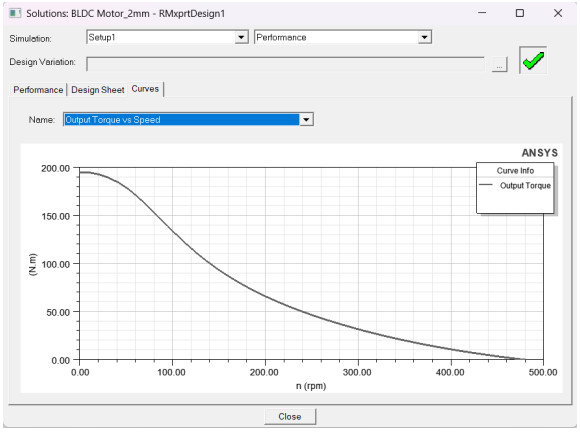

(a)

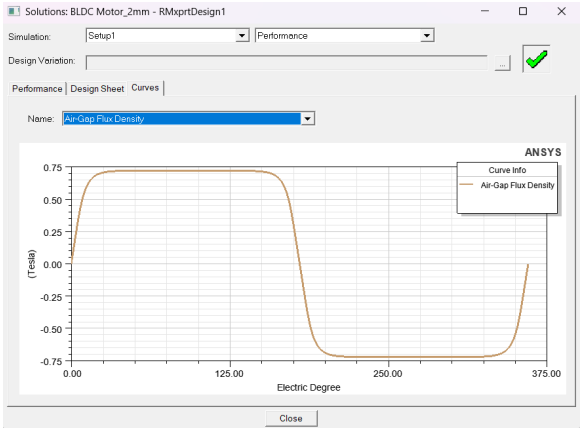

(d)

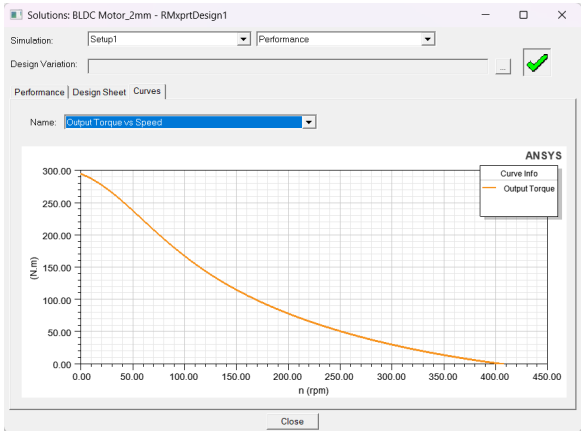

(b)

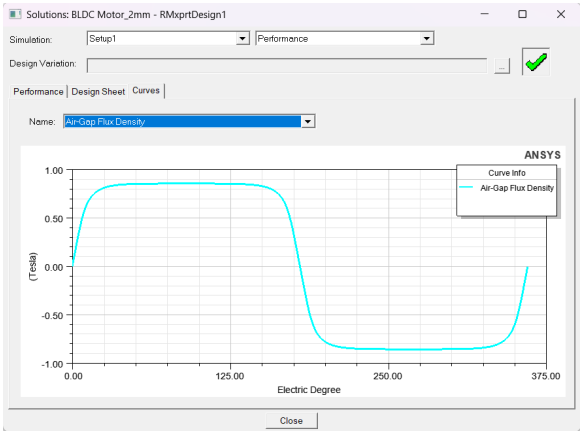

(e)

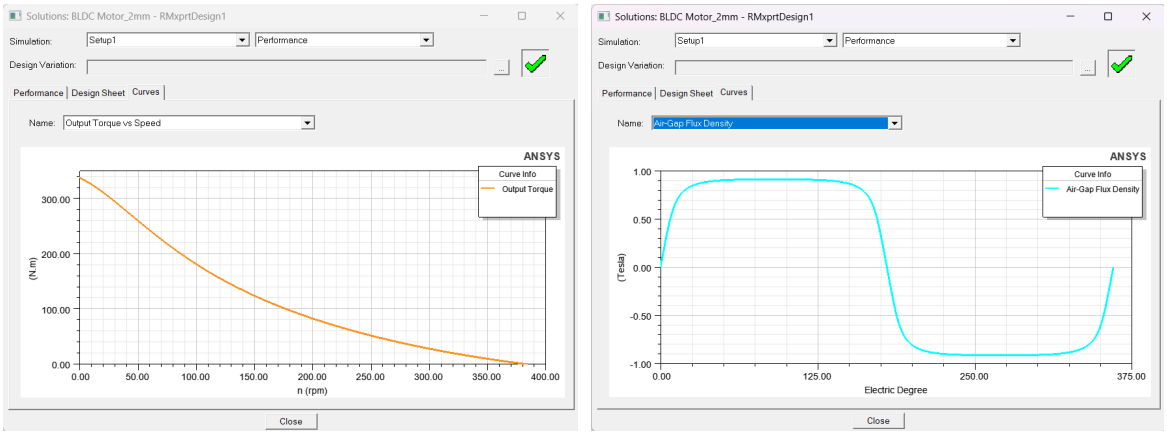

(c) (f)

Figure 9. Effects of different pole embrace ratios on motor performance: (a)-(c) Variation of cogging torque with electrical degrees (0.65, 0.80, and 0.95), (d)-(f) Air gap flux density characteristics (0.65, 0.80, and 0.95).

3.3. Stator Slot Opening and Efficiency Analysis

Reducing the stator slot openings dampens abrupt variations in air gap reluctance, thereby reducing torque ripple and ensuring smoother motor operation. However, excessive narrowing of the opening not only complicates winding insertion and increases leakage flux, leading to reduced efficiency, but also causes a resurgence in cogging torque due to local magnetic saturation occurring at the tooth tips (**Table 3**). Therefore, determining an optimum slot opening value is of critical importance for achieving both electrical efficiency and smooth operation (**Figure 10**).

In the optimized model, the stator slot opening was reconfigured to ensure that the magnetic flux density within the teeth did not exceed the 1.9 Tesla level. This modification minimized iron-core losses, particularly at high speeds. Since cogging torque tends to increase again due to magnetic saturation at narrower openings, 1.3 mm was selected as the critical value yielding the minimum cogging torque without complicating winding insertion.

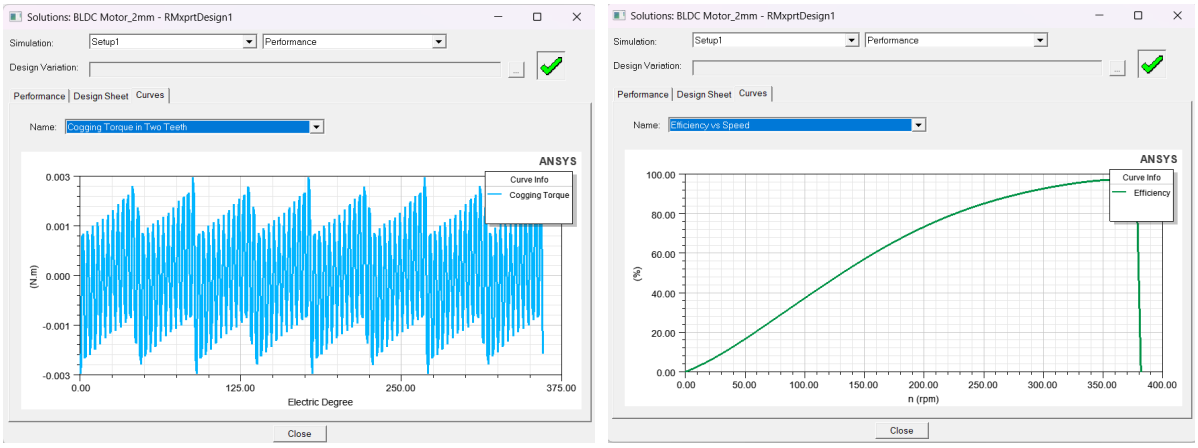

(a) (d)

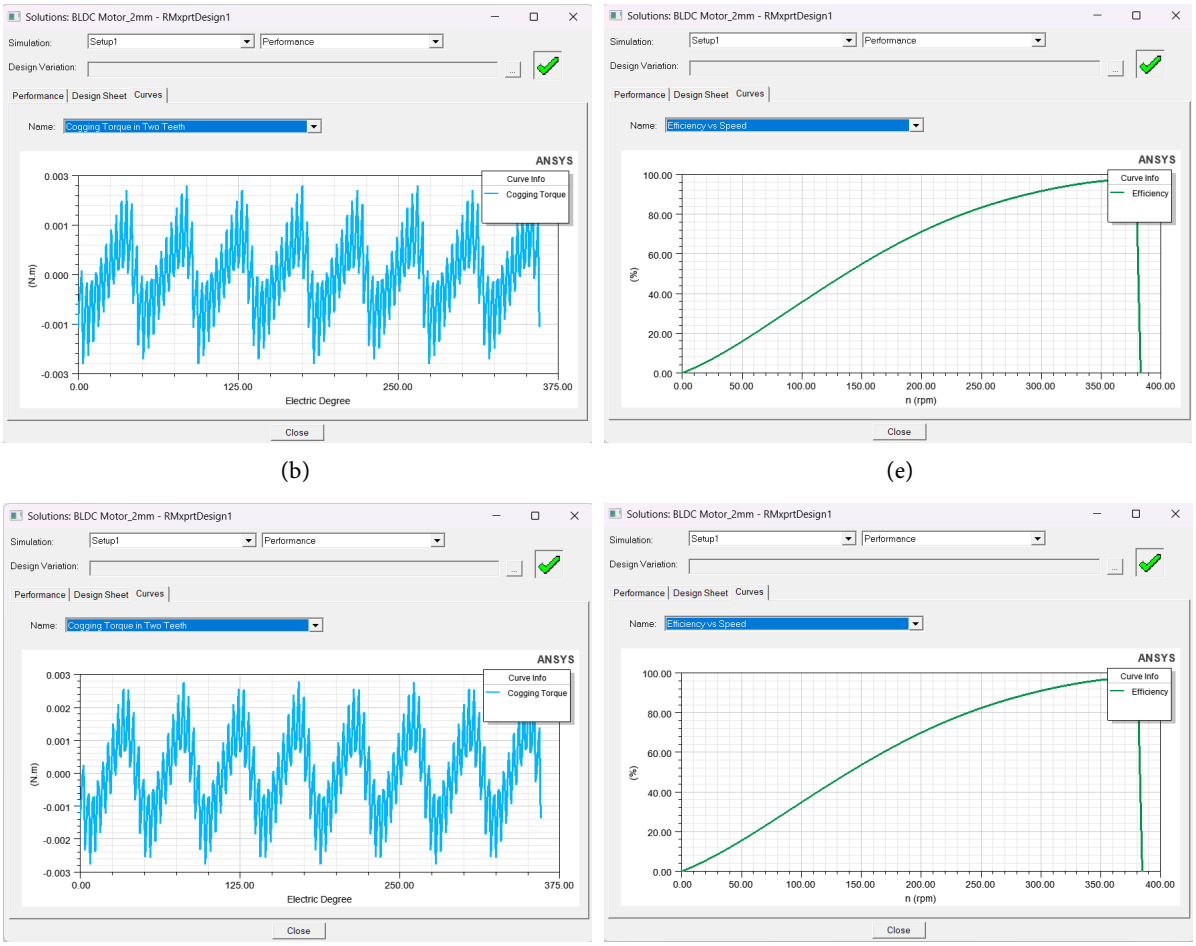

Figure 10. Effects of different stator slot openings on motor performance: (a)-(c) Variation of cogging torque with electrical degrees (1, 2, 3 mm), (d)-(f) Variation of efficiency with speed (1, 2, 3 mm).

Table 3. Effect of stator slot opening on Cogging Torque, Iron core loss, Armature copper loss, and Efficiency.

Stator slot opening (Bs0) (mm)	Cogging Torque (N·m)	Iron-Core Loss (W)	Armature Copper Loss (W)	Efficiency (%)
1	0.00246502	0.00113046	138.962	87.6311
2	0.00224072	0.00120677	124.966	88.7088
3	0.00275985	0.00124411	118.716	89.1970

3.4. Comparative Performance Evaluation

The performance data of the reference design and the final design, obtained as a result of parametric optimization, are presented comparatively in Table 4.

The comparative data presented in Table 4 clearly demonstrates the dramatic impact of the performed geometric optimization on motor performance. The most notable improvement is the 94.01% reduction achieved in cogging torque. This reduction indicates that the motor has acquired a much quieter and smoother

operational characteristic through the dampening of air gap reluctance variations. Furthermore, thanks to improvements in magnet and slot geometry, the air gap flux density was increased by 6.19%, which enabled a 0.91% rise in output torque despite a 1.66% decrease in total motor weight. The marginal decline of 1.65% observed in efficiency is evaluated as an acceptable trade-off for electric bicycle applications when compared to the increase in torque density and the radical improvement in cogging torque. Consequently, it has been numerically verified that the optimized model offers higher torque and excellent ride comfort despite being lighter.

Table 4. Comparative analysis of the reference and optimized motor.

Parameter	Reference Motor Model	Optimized Motor Model	Change (%)
Output Tork (N·m)	337.427	340.531	0.91
Cogging Torque (N·m)	0.00275985	0.000161472	−94.01
Air-Gap Flux Density (Tesla)	0.911498	0.967915	6.19
Efficiency (%)	89.197	87.7196	−1.65
Total Net Weight (kg)	3.12929	3.07753	−1.66

4. Conclusions

In this study, the effects of geometric parameters of Brushless Direct Current (BLDC) motors (magnet thickness, pole embrace ratio, stator slot structure, and air gap) on motor performance were comprehensively investigated using the Finite Element Method (FEM). Parametric analyses performed in the ANSYS Maxwell demonstrated that significant improvements in motor performance can be achieved solely through geometric optimization without increasing material costs.

The principal results obtained are summarized below:

1) *Magnetic Saturation and Sizing*: Although increasing magnet thickness initially supports torque production, it causes magnetic saturation in the stator core after a certain threshold value (3 mm for this study). This situation revealed that the perception that "thicker magnet means more torque" is not always valid and that an optimum saturation point must be targeted.

2) *Improvement in Torque Quality*: By optimizing the pole embrace ratio to 0.75 and through modifications in the stator slot geometry, the cogging torque, which is the source of vibration and noise in the motor, was reduced by 94.01% compared to the reference design. This radical reduction obtained is of a nature that directly enhances the motor's acoustic comfort and mechanical life by increasing smoothness in torque transmission.

3) *Energy Efficiency*: As a result of geometric improvements, efficiency at the nominal operating point declined from 89.19% to 87.72%. This limited decline of 1.67% is evaluated as a reasonable trade-off (Optimization Balance) in favour of ride comfort and mechanical life, considering the radical reduction in cogging torque and the increase in torque quality. An efficiency change at this level re-

mains secondary to the critical gains obtained in ride quality in electric transportation vehicles. Furthermore, the vehicle weight saving provided by lightening the motor largely compensates for the effect of this limited efficiency loss on battery range.

In conclusion, this study has confirmed the necessity of FEM-based precise geometric optimizations alongside analytical calculations in the BLDC motor design process. In future studies, it is suggested that this obtained electromagnetic design be supported by thermal analyses (Computational Fluid Dynamics-CFD) and experimentally verified through prototype production.

Conflicts of Interest

The authors declare no conflicts of interest regarding the publication of this paper.

References

[1] Jahns, T.M. and Soong, W.L. (1996) Pulsating Torque Minimization Techniques for Permanent Magnet AC Motor Drives—A Review. *IEEE Transactions on Industrial Electronics*, **43**, 321-330. https://doi.org/10.1109/41.491356

[2] Rahman, M.A. and Zhou, P. (1991) Analysis of Brushless Permanent Magnet Synchronous Motors. *IEEE Transactions on Industrial Electronics*, **43**, 256-267. https://doi.org/10.1109/41.491349

[3] Dos Santos, F.L.M. and Anazawa, R. (2023) Design Optimization Analysis on the Performance of BLDC Motors on Electric Bicycles. *International Journal of Electrical Power & Energy Systems*, **145**, Article 108620.

[4] Zhu, Z.Q. and Howe, D. (2000) Influence of Design Parameters on Cogging Torque in Permanent Magnet Machines. *IEEE Transactions on Energy Conversion*, **15**, 407-412. https://doi.org/10.1109/60.900501

[5] Park, H.I. and Lee, J. (2023) Analysis of Noise and Vibration in BLDC Motors Due to Asymmetric Air Gaps. *Journal of Mechanical Science and Technology*, **37**, 2891-2899.

[6] Zarko, D., Ban, D. and Lipo, T.A. (2006) Analytical Calculation of Magnetic Field Distribution in the Slotted Air Gap of a Surface Permanent-Magnet Motor Using Complex Relative Air-Gap Permeance. *IEEE Transactions on Magnetics*, **42**, 1828-1837. https://doi.org/10.1109/tmag.2006.874594

[7] Gundogdu, T. and Komurgoz, G. (2022) Impact of Stator Slot Shape on Cogging Torque of PMBLDC Motor. *Research in Engineering Structures and Materials*, **8**, 455-468.

[8] Upadhyay, P.K., Rajpurohit, B.S. and Kumar, R. (2023) Impact of Stator Slot Configuration and Coil Diameter on BLDC Motor Efficiency and Stability. *Technical Electrodynamics*, **4**, 45-52.

[9] Wang, D., Li, K. and Sun, Y. (2023) Effect of Slot-Pole Numbers on the Performance of a BLDC Motor for Agro-EV Application. *Machines*, **11**, Article 205.

[10] Sargın, M. and Çolak, İ. (2023) Effect of Stator Skewing on Cogging Torque and Back-EMF in BLDC Motors. *Gazi University Journal of Science*, **36**, 589-601.

[11] Wu, Y.C. and Wu, Y.T. (2025) Mitigation of Cogging Torque for Brushless Interior Permanent-Magnet Motors Using Auxiliary Slots. *Scientia Iranica*, **32**, 154-162.

[12] Bianchi, N. and Bolognani, S. (2002) Design Techniques for Reducing the Cogging

Torque in Surface-Mounted PM Motors. *IEEE Transactions on Industry Applications*, **38**, 1259-1265. https://doi.org/10.1109/tia.2002.802989

[13] Tadivaka, S. and Kumar, P. (2020) Reduction of Cogging Torque in Surface Mounted Permanent Magnet Brushless DC Motor by Adapting Rotor Magnetic Displacement. *Energies*, **13**, Article 5462.

[14] Maheshwari, P. and Pahuja, A. (2023) Effect of Pole Arc to Pole Pitch Ratio on the Performance of BLDC Motor. *International Journal of Engineering Trends and Technology*, **71**, 112-118.

[15] Noyal Doss, M.A., Ganapathy, V. and Karthikeyan, R. (2015) Cogging Torque Reduction in Brushless DC Motor by Reshaping of Rotor Magnetic Poles with Grooving Techniques. *International Review of Electrical Engineering*, **10**, 365-372.

[16] Zhao, J., Zhang, L. and Wei, J. (2024) Optimization of Magnetic Pole Shape for Reducing Torque Ripple in Surface-Mounted Permanent Magnet Motors. *IEEE Transactions on Magnetics*, **60**, 1-9.

[17] Kim, H., You, Y. and Kwon, B. (2013) Rotor Shape Optimization of Interior Permanent Magnet BLDC Motor According to Magnetization Direction. *IEEE Transactions on Magnetics*, **49**, 2193-2196. https://doi.org/10.1109/tmag.2013.2242056

[18] Liu, Y., Chen, Z. and Zhang, H. (2024) Optimization of Tangential Interior Brushless DC Motor Rotor for Hybrid Vehicles. *Scientific Reports*, **14**, Article No. 12032.

[19] Meo, S. and Vahedi, A. (2024) Comparative Studies on Performances of Slotted and Slotless High-Speed PMBLDC Motors. *IEEE Access*, **12**, 15678-15689.

[20] Atallah, K., Wang, J. and Howe, D. (2025) Torque Performance Analysis of BLDC Motor for Electric Motorcycle by Halbach and Skewing Rotor. *IEEE Transactions on Energy Conversion*, **40**, 112-120.

[21] Tibor, B., Varga, Z. and Kovacs, L. (2023). Comparative Analysis of Flux Concentration in Interior PM BLDC Motors. *Acta Polytechnica Hungarica*, **20**, 89-106.

[22] Al-Jumaili, A., Zhao, W. and Liu, X. (2025) Analysis of Stator Material Influence on BLDC Motor Performance under High Thermal Loads. *Materials*, **18**, Article 4630.

[23] Kumar, R. and Singh, S. (2020) Design and Performance Analysis of Brushless DC Motor Using ANSYS Maxwell. 2020 *IEEE International Conference on Power Electronics*, *Drives and Energy Systems*, Jaipur, 16-19 December 2020, 1-6.

[24] Lee, J., Kim, K. and Park, S. (2024) Multi-Step Design Optimization for the Improvement of an Outer-Rotor Brushless Direct Current Motor Using Taguchi Method. *Applied Sciences*, **14**, Article 4302.

[25] Islam, M.S., Mir, S. and Sebastian, T. (2005) Issues in Online Identification of Permanent Magnet Synchronous Motor Parameters. *IEEE Transactions on Industry Applications*, **41**, 72-82.